

Viscoelastic Properties of Polymer Melts from Equilibrium Molecular Dynamics Simulations

Suchira Sen,[†] Sanat K. Kumar,^{*,†} and Pawel Keblinski[‡]

Isermann Department of Chemical and Biological Engineering, and Department of Materials Science and Engineering, Rensselaer Polytechnic Institute, Troy, New York 12180

Received October 2, 2003

Revised Manuscript Received December 6, 2004

Introduction. The dynamics of polymer chains are now generally very well understood in the pioneering frameworks of the Rouse model for short chains, and the reptation model for longer chains.^{1–5} While these theories yield well-known expressions for the variation of the diffusivity D and viscosity η with the chain length N , an open question is the chain length at which one crosses over from Rouse-like behavior to reptation. This length, termed the entanglement length, N_e , is relatively easy to estimate experimentally, but has been hard to access in a simulation due to the fact that, up until recently, there was no satisfactory definition of an entanglement.^{6,7}

In numerical studies, most estimates of the entanglement length involve conducting simulations and examining dynamic quantities, such as the frequency dependent storage modulus. Extensive work has been done by Kremer and Grest⁸ to identify the onset of chain entanglement, with somewhat mixed results. Examination of the chain length dependence of chain diffusion yields a cross over from the Rouse scaling (N^{-1}) to reptation scaling (N^{-2}) behavior in the vicinity of chains of length 35. In contrast, estimates of storage modulus from nonequilibrium molecular dynamics simulations yield an entanglement chain length in the vicinity of 80.

We approach this problem with the tools of equilibrium molecular dynamics (MD).⁹ Equilibrium stress fluctuations which result naturally from these simulations directly provide estimates of the viscosity through the Green–Kubo equation, as suggested by Smith et al.¹⁰ The storage and loss modulus are also computed from the stress autocorrelation function, and the hints of a plateau are seen in the storage modulus. The plateau is the strongest indication of onset of reptation dynamics, and is seen for chain lengths of 80 and higher. Estimates of the entanglement length N_e , provide a number closer to 30, consistent with the first estimate provided by Kremer and Grest.

Simulation Model and Methods. The MD simulation employs a standard chain model. Interaction between nonbonded monomers are described by a shifted, purely repulsive Lennard-Jones (LJ) potential: $U(r) = 4\epsilon[(\sigma/r)^{12} - (\sigma/r)^6] + \epsilon$ for $r < 2^{1/6}\sigma$, and $U(r) = 0$ for $r > 2^{1/6}\sigma$. Adjacent bonded monomers interact via a stiff FENE potential, in the form of $V_{\text{FENE}} = -k(R_0^2/2) \ln(1$

Table 1. ^a

	$N = 20$	$N = 40$	$N = 80$	$N = 120$
$\langle R_e^2 \rangle (\sigma^2)$	29.2	62.6	127.5	195.1
$D (\sigma^2\tau^{-1})$	0.02	0.0074	0.0023	0.0012

^a R_e is the average end-to-end vector magnitude. D is the diffusivity.

$-(r/R_0)^2$), which constrains the distance between adjacent monomers to about 1σ (we use the same parameters for the FENE potential as Grest and Kremer in refs 5 and 8). We performed constant volume simulations of monodisperse polymer melts of varying chain lengths, and will focus our attention on the crossover regime, specifically $N = 20, 40, 80$ and 120 , respectively. In a typical simulation we use a total of 2400 monomers embedded in the periodic simulation box, of size 14.1σ in each direction, which corresponds to the reduced segment density of $\rho^* = 0.85$. In a few simulations we have doubled the number of monomers, and for the longest chain system, $N = 120$, this corresponds to increasing the number of chains from 20 to 40. Since the properties deduced from the simulation were independent of system size even for these relatively small systems, we conclude that our results only have minor finite size effects. We will report all quantities in terms of reduced units, which are defined at the end of the paper.

We conduct MD simulations using a fifth order Gear algorithm in the microcanonical ensemble with a $\delta t = 0.001t^*$ ensuring energy conservation to within 0.5% over the whole constant energy simulation run. The starting structures for our runs were constructed by gradually squeezing semidilute solutions to a final density of 0.85 over ~ 10 million MD steps at the reduced temperature, $T^* = 1$. These structures were further run at constant temperature, for an additional 10 million steps to obtain a starting configuration for the constant energy run. After the structure preparation and equilibration, we followed with the constant energy simulation for a minimum of 50 million MD steps for $N = 20$, up to 300 million MD steps for $N = 120$. The reduced temperature exhibited small (several percent) fluctuations around unity since we did not couple our simulations to a heat bath.

It is important to check our simulation results for finite-size effects. Kremer and Grest suggest that for these chain lengths a minimum number of 20 chains is required to avoid such effects. Our systems contain 2400 monomers, i.e., 20 chains for $N = 120$. In Table 1 below we have tabulated various quantities like the end-to-end vector and diffusivity, for all the chain lengths. In particular, the diffusivity, D , changed from 0.0012 to 0.0011, when the system size was doubled from 2400 to 4800 monomers. Since D is typically the most sensitive to finite size effects, and since these D values closely track the results of Kremer and Grest,⁵ we conclude that our system sizes are large enough.

To check for equilibration we use the autocorrelation function of the end-to-end vector of the chains,⁴ $\langle r_{\text{end}}(t)r_{\text{end}}(0) \rangle / \langle r_{\text{end}}^2 \rangle$, where $r_{\text{end}}(t)$ denotes the end-to-end distance vector at time t . A similar autocorrelation function can also be defined for the root-mean-square radius of gyration. Both of these autocorrelation functions showed an exponential decay, from which the

[†] Isermann Department of Chemical and Biological Engineering, Rensselaer Polytechnic Institute.

[‡] Department of Materials Science and Engineering, Rensselaer Polytechnic Institute.

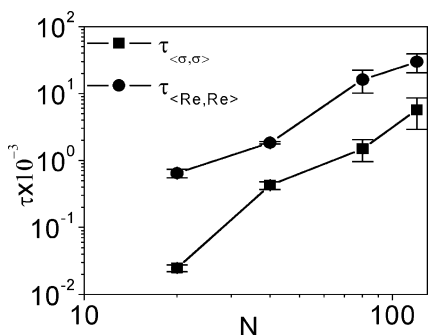


Figure 1. Relaxation time from the stress relaxation and end-to-end vector relaxation as a function of chain length.

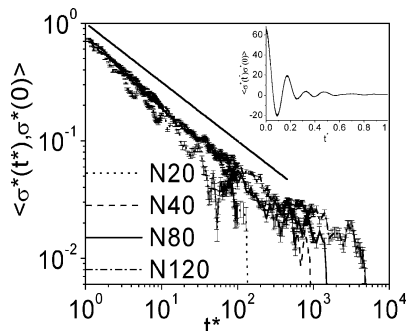


Figure 2. Stress autocorrelation function of the total stress. We stress that the intermediate time behavior of this function corresponds to a $t^{-1/2}$ scaling expected from the Rouse model (dark line), while the long time decay is well described by an exponential. Inset shows the initial part showing the short time scale fluctuations arising from bond interactions.

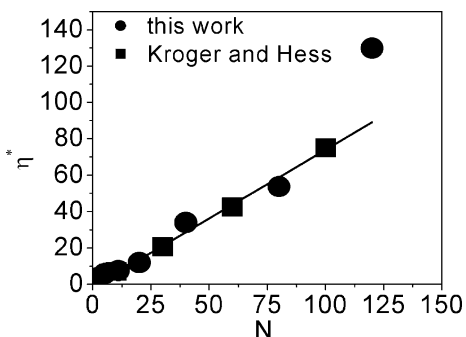


Figure 3. Plot of viscosity as a function of chain length. The line is a best fit to the viscosity for all $N \leq 100$.

equilibration time of these properties is readily obtained. Figure 1 shows that, as expected, the relaxation time of the end-to-end distance vector increases with increasing chain length. The trends from the end-to-end vector and stress relaxation seem to be different for $N = 20$, but the two curves track each other for all longer chains.

Calculation of the zero shear rate viscosity using the Green–Kubo formula requires the stress autocorrelation function (acf). The stress acfs are plotted in Figure 2. We calculate the stresses through the use of the atomic virial defined as $\sigma_{ij} = (1/V)[-nk_B T \delta_{ij} + \sum_{\alpha} (r_{\alpha}^{-1} U'_{\alpha}(r_{\alpha}) r_{\alpha i} r_{\alpha j})]$, where σ_{ij} is the stress for atom pair ij . The first term is the kinetic energy contribution while the second term accounts for all bonded and nonbonded interactions (α is thus a summation over all atom pairs in the system). Comparison of our approach with existing literature (see Figure 3) suggests that our methodology is accurate for the calculation of transport properties. The acfs of the three off-diagonal elements of the stress tensor are expected to be equivalent due to the

isotropy of the system, and hence these are averaged to improve their signal. Even after several hundred million simulation steps, the resulting correlation functions are found to be noisy. The most common procedure for noise reduction in stochastic processes is averaging over several independent data sets. However, we found that beyond a certain threshold, additional averaging does not reduce the noise. The signal at this point is still very noisy, which indicates that the intrinsic noise level in the system is very high. We suspect the noise arises from numerical precision issues, at the small magnitudes of the stress correlation function, especially at long times. So a running average was performed. This average for each time t , was defined as the average from $0.9t$ to $1.1t$. This procedure preserves the fine features of the correlation function at short times and at the same time significantly reduces the noise at large times. Additionally, since the data for the two different system sizes for $N = 120$ were found to superpose we additionally averaged them to improve the signal-to-noise concerns.

Results. In Figure 2 (inset) we see that the stress acf has short time, oscillatory behavior. This is attributed primarily to the rapid fluctuations of the stiff bond potential. The long time behavior arises from the Rouse like dynamics of the single chain and any chain–chain interactions. In particular, the intermediate time scale behavior of the stress acf is consistent with the Rouse model scaling, $t^{-1/2}$, while the long time decay is exponential, with a time constant characterizing the longest stress relaxation time in the system. It is clear that the longest relaxation time from the stress autocorrelation function (see Figure 1) follows the same power law scaling with N as the end-to-end vector relaxation time at least for $N \geq 40$. However, surprisingly, the stress relaxation time is about an order of magnitude smaller than the end-to-end distance relaxation time. This result may be a consequence of the fact that the end-to-end acf only decays to zero when the orientations trudecorrelate in space (i.e., both in magnitude and orientation), while the stress correlation function is related to only that fraction of stress that has remained unrelaxed. We conclude that orientational decorrelation may be too restrictive a requirement for stress relaxation.

The viscosity is obtained using the Green–Kubo relationship: $\eta^0 = (V/k_B T) \int_0^{+\infty} \langle \sigma_{xy}(t) \sigma_{xy}(0) \rangle dt$. It is plotted as a function of N in Figure 3. Our results are in good agreement with the data from Kroger and Hess¹¹ who performed NEMD simulations over a range of strain rates, and extrapolated to the zero shear limit. However, it should be noted that their system had a density, $\rho^* = 0.84$, while the density of our system is $\rho^* = 0.85$. Note that the viscosity appears to vary linearly with N for $N \leq 100$, while the $N = 120$ simulation has a distinctly larger viscosity. On this basis one might argue that the first dynamic manifestations of entanglement are only felt for $N > 100$: we shall discuss this point further below.

The stress acf is also used to generate the complex, frequency-dependent modulus of the melt. The relation between the moduli and the stress acf is

$$G^*(\omega) = G'(\omega) + iG''(\omega) = i\omega \frac{V}{k_B T} \int_0^{+\infty} e^{-i\omega t} \langle \sigma_{xy}(t) \sigma_{xy}(0) \rangle dt \quad (1)$$

115
116
117
118
119
120
121
122
123
124
125
126
127
128
129
130
131
132
133
134

135
136
137
138
139
140
141
142
143
144
145
146
147
148
149
150
151
152
153
154
155
156
157
158
159
160
161
162
163
164
165
166
167
168
169
170
171
172
173
174
175
176
177
178
179
180
181
182
183
184
185
186
187
188
189
190
191
192
193
194
195
196

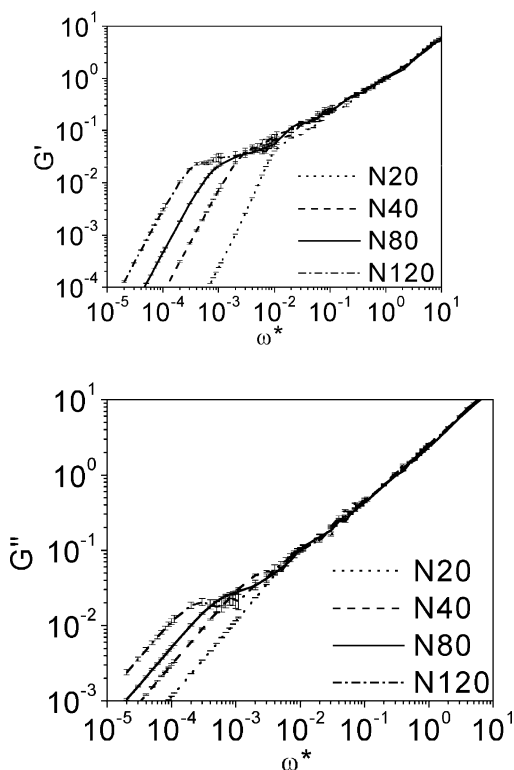


Figure 4. Storage and loss moduli as a function of reduced frequency for different chain length melts.

We plot $G'(\omega)$ and $G''(\omega)$, the storage and loss modulus, respectively, as a function of reduced frequency, ω^* , in Figure 4. Both moduli were obtained via a numerical integration of the acfs, which have been smoothed by the running average procedure described above. For $N \geq 80$, we find that $G'(\omega)$ shows evidence for an entanglement plateau, a result which is even clearer for the $N = 120$. The plateau modulus for $N = 120$ is found to be $G_N^0 = 0.03$. The entanglement chain length can then be estimated from the theory of rubber elasticity: $N_{e,p} = (\rho k_B T / G_N^0)$. We find $N_{e,p} = 28$. This number is close to the value of 32 obtained by Kremer and Grest from diffusion coefficient and also the relaxation times of the melts.^{5,8} However, NEMD simulations report a much higher value for the $N_e \approx 80$, but Kremer and Grest suggest that these higher numbers might only be obtained for much longer chains. Previous experimental results of Richter,¹² using neutron spin-echo studies of the dynamic structure factor, report an $N_e = 30$. The precise definition of the entanglement length is thus unresolved, and we argue that this matter can be addressed only by conducting equilibrium simulations on truly long chains.

Discussion. Two issues bear more discussion. First, the two different estimates for the entanglement molecular weight obtained from our simulations and those of Kremer and Grest need to be reconciled. Second, we need to understand why the viscosity appears to vary linearly with chain length even in the regime where the chains are clearly longer than the entanglement threshold.

To understand the second point, we decompose the viscosity into three components: (i) the early time oscillatory contribution; (ii) the Rouse contribution where the stress relaxation varies inversely with the square root of time; (iii) the exponential contribution that governs the longest relaxation time of the stress

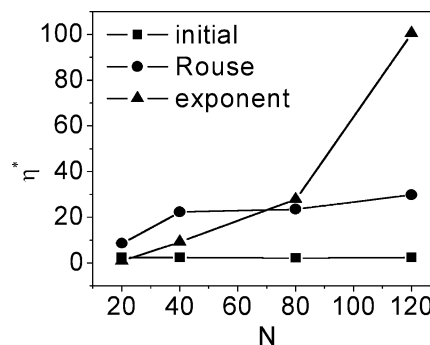


Figure 5. Different contributions to the viscosity as discussed in the text.

acf. Figure 5 shows these three contributions as a function of chain length. We find that the contribution from the first section is small and independent of N as expected, because it comes from the bond vibrations and is hence independent of chain length. The Rouse contribution to the viscosity varies linearly with N , again, as expected for short chains. But its percentage contribution to the total viscosity decreases, since the contribution from the longest relaxation time increases strongly with N . Note that the Rouse contribution appears to plateau above $N = 40$, clearly signaling the addition of extra mechanisms to the dynamics, beyond simple Rouse. This is consistent with our estimate of an entanglement length of 28, and also with the notion that chain motion is only Rouse like between entanglement points. The steep scaling of viscosity, beyond the linear regime, clearly comes from the terminal drop-off region. Even though the contribution from the longest relaxation time increases strongly with N , it only becomes comparable to the Rouse contribution at a chain length of $N = 80$. Thus, even though the chains are completely out of the Rouse regime and in the entangled region by that chain length, one still has to go to much higher chain lengths before the viscosity scaling with chain length is perceptibly different from the Rouse scaling.

Next we focus on resolving the apparent discrepancies between the different simulation estimates of the entanglement chain length. First, our estimates of the entanglement length are consistent with those derived from the crossover of the diffusion scaling from the Rouse regime to reptation reported previously by Kremer and Grest.⁸ Since these estimates are derived from relatively short chain lengths, it is reassuring that they agree. In contrast, the simulations of Grest and Kremer yield estimates for the elastic modulus of truly long chains ($N > 350$) which are about a factor of 2–3 smaller than our plateau values. Consequently, Kremer and Grest find larger values for the entanglement length. While these results would suggest that a very strong finite chain size effect is in play here, as has been conjectured by Kremer and Grest,⁸ experimental results suggest that the plateau modulus, if anything, increases with increasing chain length. On this basis, we conjecture that our estimate is an underestimate rather than overestimate the value of the plateau for longer chains.¹³ We point to the fact that the Kremer–Grest estimates were from simulations where the melt is initially stretched by a large amount and then allowed to relax to equilibrium. It is unclear to us if these results yield the zero shear storage modulus corresponding to the entanglement plateau or if these estimates correspond to the shear thinning regime. If these simulations were

197
198
199
200
201
202
203
204
205
206
207
208
209
210
211
212
213
214
215
216
217
218
219
220
221
222
223
224
225
226
227
228
229
230
231
232
233

234
235
236
237
238
239
240
241
242
243
244
245
246
247
248
249
250
251
252
253
254
255
256
257
258
259
260
261
262
263
264
265
266
267
268
269
270
271
272
273
274
275
276
277
278
283
284
285
286

287 in the shear thinning regime, as might be expected from
 288 the simulation of Kroger and Hess,¹² then the resulting
 289 elastic plateau moduli would be too small, thus resulting
 290 in high estimates of the entanglement chain length.
 291 With all these points, it is appropriate to conclude that
 292 the numerical value of entanglement length is only
 293 known to certainty to within a factor of 2: more
 294 conclusive equilibrium MD simulations for much longer
 295 chains are necessary, and are currently being conducted,
 296 to unequivocally resolve these issues.

297 **Conclusions.** We have conducted equilibrium MD
 298 simulations to determine the stress relaxation of poly-
 299 mer melts in the crossover regime between Rouse and
 300 reptation, and find that the storage modulus and the
 301 stress autocorrelation function appear to show signa-
 302 tures consistent with reptation dynamics, especially for
 303 chains longer than $N = 80$. We estimate an entangle-
 304 ment chain length of 28 from the value of the storage
 305 modulus plateau, which is consistent with previous
 306 estimates from equilibrium chain diffusion simulations
 307 and experiment, but not with more recent nonequilib-
 308 rium simulations of Kremer and Grest. The entangle-
 309 ment length is thus only known to within a factor of 2.
 310 A surprising result, which is potentially important for
 311 the simulation of the mechanical properties of polymer
 312 melts, is that the longest relaxation time for the stress
 313 acf is several times smaller than those estimated from
 314 acf of structural quantities, such as the end-to-end
 315 distance acf.

316 **Acknowledgment.** We thank Gary Grest for useful
 317 discussions. Financial support for this work was pro-
 318 vided by the Office of Naval Research Contract No.
 319 N00014-01-10732 (P.K.; S.K.K.), the National Science
 320 Foundation (DMR-01xxx; S.K.K.), and the National

Science Foundation Nanoscale Science and Engineering 321
 Center at RPI, NSF Grant No. DMR-0117792 (S.K.K.; 322
 P.K.). 323

Nomenclature 324

length parameter: σ	325
well depth in LJ interaction: ϵ	326
reduced time: $t^* = t/\tau$; $\tau = \sigma\sqrt{m/\epsilon}$	327
reduced temperature: $T^* = (k_B T/\epsilon)$	328
reduced density: $\rho^* = 0.85 = \rho\sigma^3$	329
reduced viscosity: $\eta^* = \eta/k_B T\sigma^{-3}\tau$	330
reduced stress correlation: $\langle\sigma_{xy}^*(\tau)\sigma_{xy}^*(0)\rangle = \langle\sigma_{xy}(\tau)\sigma_{xy}(0)\rangle/k_B T\sigma^{-3}$	331 332
reduced plateau modulus: $G_N^0 = G_N/k_B T\sigma^{-3}$	333
reduced frequency: $\omega^* = \omega\tau$	334

References and Notes 335

- (1) de Gennes, P. G. *Scaling Concepts in Polymer Physics*; 336
Cornell University Press: Ithaca, NY, 1979. 337
- (2) Doi, M.; Edwards, S. F. *The Theory of Polymer Dynamics*; 338
Clarendon: Oxford, U.K., 1986. 339
- (3) Kreer, T.; Baschnagel, J.; Muller, M.; Binder, K. *Macromol-* 340
ecules **2001**, *34*, 1105. 341
- (4) Paul, W.; Binder, K.; Heermann, D. W.; Kremer, K. *J. Chem.* 342
Phys. **1991**, *95*, 7726. 343
- (5) Kremer, K.; Grest, G. *J. Chem. Phys.* **1990**, *92*, 5057. 344
- (6) Padding, J. T.; Briels, W. J. *J. Chem. Phys.* **2002**, *117*, 925. 345
- (7) Everaers, R.; Sukumaran, S. K.; Grest, G. S.; Svaneborg, 346
C.; Sivasubramian, A.; Kremer, K. *Science* **2004**, *303*, 823. 347
- (8) Putz, M.; Kremer, K.; Grest, G. *Europhys. Lett.* **2000**, *49*, 348
735. 349
- (9) Gao, J.; Weiner, J. H. *J. Chem. Phys.* **1995**, *103*, 1621 and 350
references therein. 351
- (10) Bedrov, D.; Smith, G. D.; Douglas, J. F. *Europhys. Lett.* 352
2002, *59*, 384. 353
- (11) Kroger, M.; Loose, W.; Hess, S. *J. Rheol.* **1993**, *37*, 1057. 354
- (12) Wischenwski, A.; Richter, D. *Europhys. Lett.* **2000**, *52*, 719. 355
- (13) Onogi, S.; et. al. *Macromolecules* **1970**, *3*, 109. 356

MA035487L

357